Novel Hybrid Electrocatalyst with Enhanced Performance in Alkaline Media: Hollow Au/Pd Core/Shell Nanostructures with a Raspberry Surface

Zhelin Liu,[†,‡] Bo Zhao,[§] Cunlan Guo,[†,‡] Yujing Sun,[†,‡] Fugang Xu,[†,‡] Haibin Yang,[§] and Zhuang Li*[,†]

State Key Laboratory of Electroanalytical Chemistry, Changchun Institute of Applied Chemistry, Chinese Academy of Sciences, Changchun, Jilin 130022, People's Republic of China, Graduate School of the Chinese Academy of Sciences, Beijing 100039, People's Republic of China, and State Key Laboratory of Superhard Materials, Jilin University, Changchun 130012, People's Republic of China

Received: May 28, 2009; Revised Manuscript Received: July 29, 2009

In this paper, a hollow Au/Pd core/shell nanostructure with a raspberry surface was developed for methanol, ethanol, and formic acid oxidation in alkaline media. The results showed that it possessed better electrocatalyst performance than hollow Au nanospheres or Pd nanoparticles. The nanostructure was fabricated via a two-step method. Hollow Au nanospheres were first synthesized by a galvanic replacement reaction, and then they were coated with a layer of Pd grains. Several characterizations such as transmission electron microscopy (TEM), scanning electron microscopy (SEM), energy-dispersive X-ray spectroscopy (EDX), and X-ray photoelectron spectroscopy (XPS) were used to investigate the prepared nanostructures. The intensive studies of fuel cells encouraged us to examine the electrocatalytic properties of the prepared nanostructures, and that alkaline media could supply a more active environment than acidic electrolyte in previous reports inspired us to operate the experiments in alkaline media. According to the results, this hollow Au/Pd core/shell nanostructure with a raspberry surface possesses excellent electrocatalytic properties and can be further used in direct alcohol/formic acid fuel cells (DAFCs or DFAFCs), sensors, and catalysts.

1. Introduction

As a novel technique for hydrogen energy application, fuel cells have been widely studied due to their advantages such as high efficiency and cleanness. In recent years, organic materials such as methanol, ethanol, and formic acid have aroused increasing attention for their high potential as fuel cell candidates. Therefore, the electrooxidation of these materials[1−7] has been intensively studied due to their potential applications in fuel cells. With the development of nanotechnology, nanostructures provide more opportunities for searching or designing an effective catalyst. Among numerous nanocatalysts, Pt-based catalysts were considered to be the best in low-temperature fuel cells.[8] A great number of literature citations have been reported to design unsupported or supported Pt catalyst. However, the high cost and limited source of Pt narrowed its use.[9] Some reports have pointed out that if DAFCs could be operated in an alkaline media rather than an acid electrolyte, reaction kinetics would be significantly improved and non-Pt electrocatalysts could be employed simultaneously.[10−13] Recently, Pd-based electrocatalysts, as one of the non-Pt electrocatalysts, have been found to possess prominent properties for catalyzing alcohol or formic acid, and developed for alcohol electrooxidation in alkaline media.[14−16] To the best of our knowledge, electrooxidation of formic acid in alkaline media for Pd-based catalysts has not been reported yet.

On the other hand, considerable attention has been paid to noble metal nanostructures due to their potential applications in many areas, such as SERS, catalysis, information storage, biosensing, and so on.[17−23] The morphology effect of the noble metal used as a catalyst has driven people into synthesizing different morphologies with more and more interest. Among them, noble metal nanomaterials with hollow nanostructure were found to possess the potential for further cost savings. Meanwhile, they have also been exploited to exhibit prominent catalytic properties with the advantages of low density and high surface area.[19,24,25] In commonly used methods, materials with hollow nanostructures were usually fabricated by using a sacrificial template, such as silica spheres[26,27] and polystyrene spheres,[28,29] followed by the removal of the template, which made the process complicated and limited their use. The galvanic replacement reactions involving desired metal ions and sacrificial metal nanoparticles provided a simple route to the facile synthesis of hollow noble metal nanostructures.[30] For example, hollow Pt,[19] Au,[31−33] Ag,[34] Pd,[35] Au/Pt alloy,[36] Au/Pt core/shell,[37] and Au/Ag double-shell[38] nanostructures have been prepared in this way, which sacrificed Co nanoparticles as the templates in the replacement reactions.

Combining the advantages of both Pd and hollow structure as potential catalysts in fuel cells, here we designed a facile, efficient, and economic route to synthesize novel Pd-coated-Au hollow nanostructures with a raspberry surface. Hollow Au nanospheres were first prepared via the galvanic replacement reaction involving Co nanoparticles and $HAuCl_4$ without the protection of nitrogen. Then the surface of hollow Au nanospheres was covered with a layer of Pd grains, forming a raspberry exterior. To the best of our knowledge, the fabrication of this nanostructure and its electrochemical properties have been rarely reported. We found that this raspberry hollow Au/Pd nanostructure showed enhanced catalytic properties for methanol, ethanol, and formic acid electrooxidation in alkaline media

* To whom correspondence should be addressed. Phone/fax: +86 431 85262057. E-mail: zli@ciac.jl.cn.
† Chinese Academy of Sciences.
‡ Graduate School of the Chinese Academy of Sciences.
§ Jilin University.

10.1021/jp905007r CCC: $40.75
Published on Web 08/31/2009

in comparison with hollow Au nanospheres or Pd nanoparticles, and possessed potential applications in constructing DAFCs or DFAFCs.

2. Experimental Methods

2.1. Materials. Chemicals like cobalt chloride ($CoCl_2 \cdot 6H_2O$), citric acid, ascorbic acid (Vitamin C), chloroauric acid ($HAuCl_4 \cdot 3H_2O$), palladium chloride ($PdCl_2$), poly(*N*-vinyl-2-pyrrolidone) (PVP, K30), ethanol, sodium borohydride, hydrochloric acid, nitric acid, methanol, formic acid, and potassium hydroxide were all of analytical grade and used as received without further purification. The water used throughout all experiments was ultrapure of resistivity no less than 18.2 MΩ cm.

2.2. Synthesis of Hollow Au Nanospheres. Hollow Au nanospheres were simply synthesized analogous to the literature previously reported with a slight modification.[32,33] Briefly, 0.01 g of citric acid and 0.015 g of $NaBH_4$ were dissolved in 50 mL of water, followed by injecting 50 μL of 0.4 M $CoCl_2$ solution to form a brown solution. When the bubbles ceased, 1.1 mL of 12 mM $HAuCl_4$ aqueous solution was then mixed with the above solution with rapid agitation. The resulting solution was then stirred for 30 min and kept in ambient condition for further use. The whole process was carried out without the protection of nitrogen. The product was centrifuged and washed with water.

2.3. Synthesis of Hollow Au/Pd Core/Shell Nanostructures. Prior to the synthesis, a 56.4 mM H_2PdCl_4 solution was obtained by the following steps: A 1 g sample of $PdCl_2$ was dissolved in 36 mL of 0.2 M HCl aqueous solution and then diluted to 100 mL volume with water. In a typical synthesis, 10 mL of the prepared hollow Au nanospheres was placed in a beaker, and then mixed with 200 μL of 56.4 mM H_2PdCl_4 solution. After stirring for a while, 300 μL of 0.1 M ascorbic acid was added dropwise, and the resulting solution was stirred for 30 min and kept in ambient condition for further use. The product was centrifuged and redispersed in water.

2.4. Synthesis of Pd Nanoparticles. In this study, Pd nanoparticles were prepared according to a method previously reported.[39] In brief, 50 mL of a mixture of aqueous H_2PdCl_4 (4.0 mM, 7.5 mL, 30 μmol of Pd), ethanol (10 mL), water (32.5 mL), and PVP (30 μmol) was heated at reflux temperature (100 °C) in a 100 mL flask for 3 h under air to synthesize the PVP-protected Pd nanoparticles.

2.5. Apparatus. The samples for TEM, SEM, EDX, and XPS characterization were prepared by placing a certain amount of prepared solution on a carbon-coated copper grid and silicon wafers before drying at room temperature, respectively. TEM images were recorded by a HITACHI H-8100 EM operated at an accelerating voltage of 200 kV. The SEM and EDX data were obtained on a XL30 ESEM FEG scanning electron microscope equipped with an energy-dispersive X-ray analyzer at an accelerating voltage of 20 kV. XPS measurement was performed on an ESCALAB-MKII spectrometer (United Kingdom) with Al Kα X-ray radiation as the X-ray source for excitation. UV−visible absorbance spectra were measured with a CARY 500 Scan UV−vis−near-infrared (UV−vis−NIR) spectrophotometer.

2.6. Electrochemical Measurements. Electrochemical measurements were performed with a CHI 660A electrochemical analyzer (CH Instruments, Chenhua Co., Shanghai, China). All measurements were conducted on a conventional three-electrode cell, which includes a Ag/AgCl electrode (saturated KCl) as reference electrode, a platinum wire as counter electrode, and a bare or modified glassy carbon (GC) electrode (3 mm in diameter) as working electrode. In these experiments, the GC electrode was first carefully polished to mirror, and a certain amount of desired solution (10 μg) was pipetted onto the GC electrode and allowed to dry under an infrared lamp. Then, 10 μL of Nafion (0.05 wt %) was dropped on the surface of the modified electrode. The methanol or ethanol electrooxidation experiments were measured in 0.5 M KOH containing 0.5 M methanol or ethanol at a scan rate of 50 mV s^{-1}. The cyclic voltammetric (CV) experiments for catalyzing formic acid were carried out in 0.5 M KOH containing 0.5 M formic acid when the scan rate was 50 mV s^{-1}, and N_2 was bubbled for 20 min prior to starting the experiments.

3. Results and Discussion

Panels a and b of Figure 1 show the typical TEM and SEM images of the hollow Au nanospheres. As noted in Figure 1a, all nanospheres obviously have a center much brighter than the edge, confirming the hollow interiors. Counting on 200 nanoparticles in Figure 1b, the average outer and inner diameters of the hollow Au nanospheres are measured to be approximately 35 and 17 nm. Panels c and d of Figure 1 are the TEM and SEM images of the prepared hollow Au/Pd core/shell nanostructures. The fabrication of the nanostructure is a typical seed growth process. As the TEM images noted in Figure 1c, it can be obviously observed that a layer of grains is deposited on the surface of each hollow Au nanosphere, showing a much brighter edge outside the dark nanoshell, forming a raspberry core/shell nanostructure. Besides, the cavity in each nanostructure can also be distinguished by the contrast in Figure 1c. Note that the cavities in Figure 1c are vaguer than in Figure 1a due to the possible reason of decreased light permeation caused by the growth of the Pd layer. Figure 1d shows the typical SEM images, in which the size of the nanostructures can be estimated to be about 45 nm, and by comparing with the 35 nm obtained from Figure 1b, the formation of the Pd nanoshells outside the Au hollow nanospheres can be suggested.

EDX was employed to identify the chemical composition of the prepared nanostructure. As shown in Figure 2, two main peaks ascribed to Au and Pd are observed (a much higher peak originates from silicon wafer, a lower peak near 3 keV is also assigned to Pd), indicating the nanostructure is composed of metallic Au and Pd. Besides that, the weight ratio of Pd to Au was nearly 1:1 (not shown), which was lower than the ratio that we put in. XPS is helpful for detecting the surface composition of samples, and is further used to investigate the chemical composition of the nanostructure. The Pd 3d region and Au 4f region in the XPS spectrum of the nanostructure are illustrated in panels a and b of Figure 3. The peaks in Figure 3a at binding energies of 335.75 and 340.95 eV can be ascribed to Pd $3d_{5/2}$ and $3d_{3/2}$, respectively, which are in accordance with those reported for metallic Pd.[40] Besides that, very weak Au 4f signals characteristic of metallic Au (Figure 3b) are observed, suggesting the hollow Au nanospheres are embedded beneath the Pd layers, and the signals may come from the interstices of Pd grains. In comparison, the XPS spectrum of hollow Au nanospheres is also shown in Figure 3c, in which the intensity is nearly 15 times higher than that in Figure 3b, further supporting something exists outside the hollow Au nanospheres. By combining with EDX, it can be indicated that Pd is successfully grown on the surface of the hollow Au nanospheres, forming a core/shell nanostructure.

As is known, UV−vis spectroscopy can investigate the surface plasmon resonance (SPR) property that is commonly used to monitor the growth of the Pd shell on the hollow Au nanospheres. The UV−vis spectra of the as-prepared hollow Au nanospheres and Au/Pd nanostructures are shown in Figure

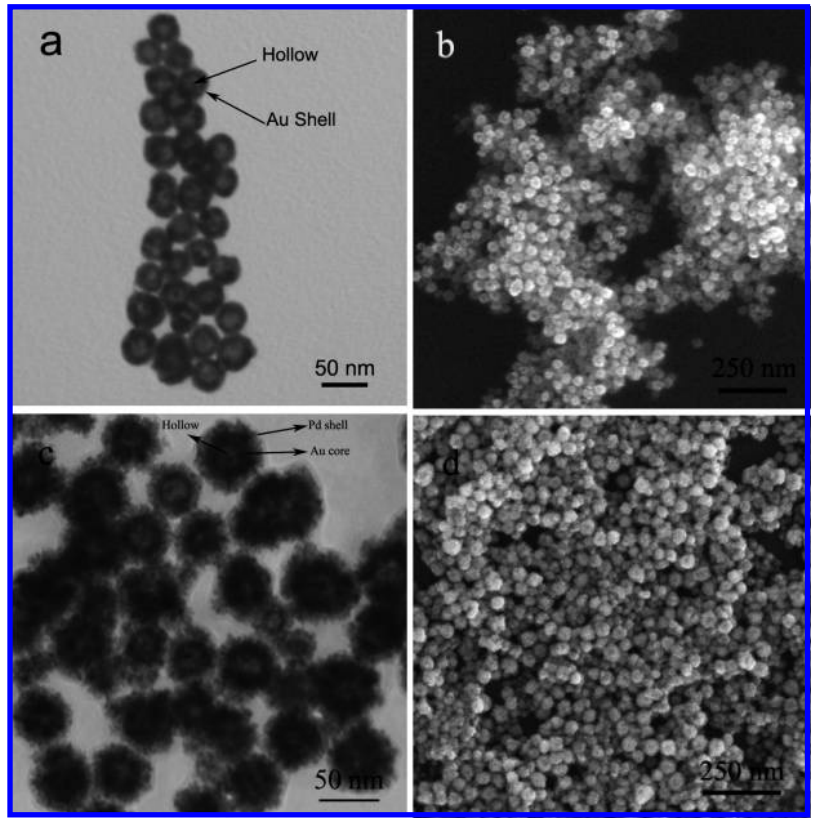

Figure 1. Typical TEM (a) and SEM (b) images of hollow Au nanospheres. Typical TEM (c) and SEM (d) images of the prepared hollow Au/Pd nanostructures with a raspberry surface.

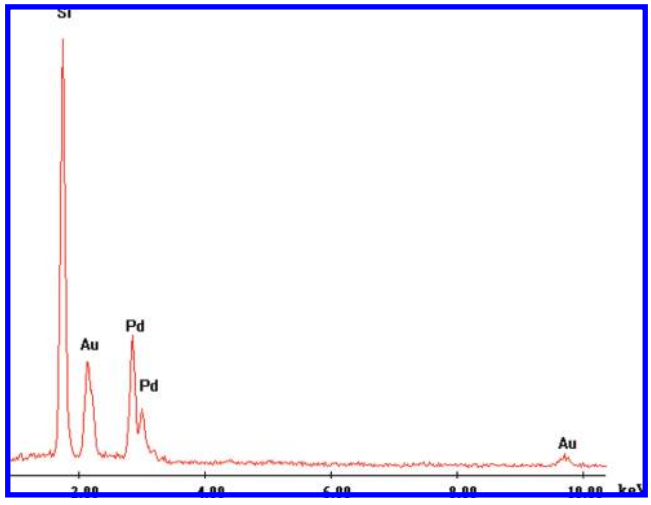

Figure 2. EDX image of the prepared hollow Au/Pd nanostructures.

4. It is obvious that the solution manifests the SPR peak characteristic of hollow Au nanospheres at 570 nm in Figure 4a. The red-shift of the SPR peak should be assigned to the hollow cavity of the nanospheres, which is in accordance with the literature reported previously.[33] However, after a layer of Pd grains grows on the hollow Au nanospheres, the SPR of hollow Au/Pd nanostructures does not show any adsorption peak in the investigated region (Figure 4b). This may be attributed to the reason that the Pd shell does not have any characteristic absorption in the UV−vis−NIR spectroscopy, and the Pd shell in the as-prepared Au/Pd nanostructure is thick enough to hide the characteristic SPR peak of the hollow Au nanosphere. This can be another support for the formation of the core/shell nanostructure. Another fact may also be responsible for the spectrum, that is, changing the dielectric surrounding the Au could be an important factor as well as the large scattering by the Pd shell.[41]

The mechanism can be summarized according to the characterizations discussed above. A two-step route is employed in this fabrication. Details are shown as a schematic illustration in Figure 5. Hollow Au nanospheres were first fabricated via employing Co nanoparticles as templates. Comparing with the hollow Au nanospheres fabricated previously,[32,33] the hollow Au nanospheres here were prepared without the protection of nitrogen. Co nanoparticles used here were prepared by reducing Co^{2+} by $NaBH_4$. Although the major products from the reduction are always Co_2B (eq 1), the metallic Co can be formed during the sacrificial oxidation/reduction reaction (eq 2).[42] The dissolving of O_2 in the solution can provide the required O_2 for eq 2. The galvanic replacement reaction has been utilized in several syntheses of inorganic hollow nanostructures. The driving force of the galvanic replacement reaction originates from the large gap between reduction potentials of $AuCl_4^-$/Au and Co^{2+}/Co. Since the reduction potential of the $AuCl_4^-$/Au redox couple (0.935 V vs. SHE) is much higher than that of the Co^{2+}/Co redox couple (−0.377 V vs. SHE), $AuCl_4^-$ will be reduced to Au atoms (eq 3) as soon as $AuCl_4^-$ ions contact with metallic Co and hollow Au nanospheres form. Subsequently, when H_2PdCl_4 was added to the solution in the presence of ascorbic acid, $PdCl_4^{2-}$ was reduced gradually to form metallic Pd. As the lattices of Au and Pd are reasonably similar, the interfacial energy is relatively low between them. Therefore, metallic Pd should deposit on the already existing surface of hollow Au nanospheres instead of self-nucleating in the solution.[43−47] On the other hand, because ascorbic acid is a kind of weak reductant, and the experiments were carried out under room temperature, H_2PdCl_4 should be reduced to Pd nanoparticles.

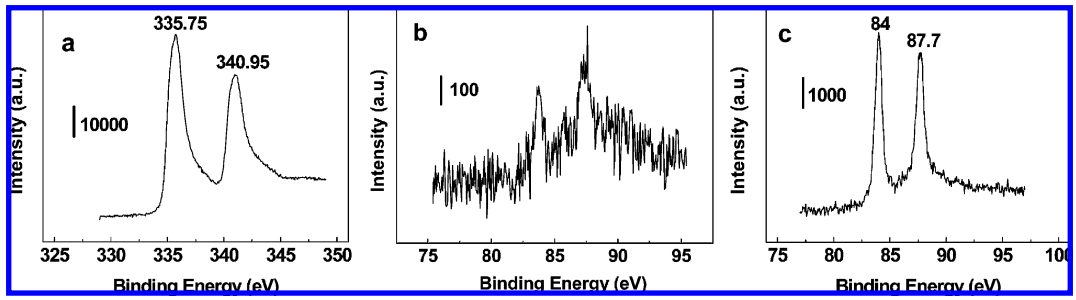

Figure 3. XPS spectra of the prepared hollow Au/Pd nanostructures (a: Pd 3d region; b: Au 4f region) and hollow Au nanospheres (c).

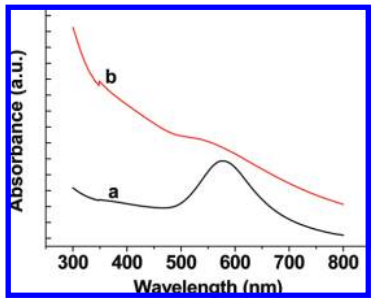

Figure 4. UV−vis spectra of as-prepared hollow Au nanospheres (a) and the prepared hollow Au/Pd nanostructures (b).

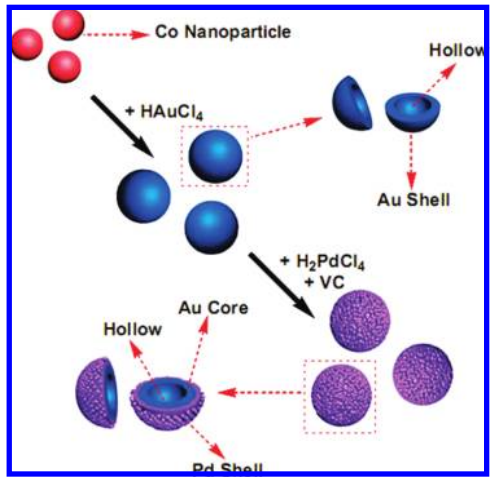

Figure 5. Schematic illustration of the formation process of Au/Pd hollow nanostructures.

Note that the reaction condition was not furious enough to reduce all $PdCl_4^{2-}$, which was in agreement with the EDX data.

$$2Co^{2+} + 4BH_4^- + 9H_2O \rightarrow Co_2B + 12.5H_2 + 3B(OH)_3 \quad (1)$$

$$4Co_2B + 3O_2 \rightarrow 8Co + 2B_2O_3 \quad (2)$$

$$3Co + 2AuCl_4^- \rightarrow 2Au + 3Co^{2+} + 8Cl^- \quad (3)$$

Using nanoparticle-modified electrodes has noteworthy advantages, such as large surface area, unique morphology, small size, increased mass transport, and possible increased electronic interaction between metal nanoparticles and reactant molecules. Since this as-prepared raspberry hollow Au/Pd nanostructure was considered to possess enhanced electrochemical activity due to its peculiar structure, we applied the as-prepared nanostructure to be deposited onto the surface of GC electrodes

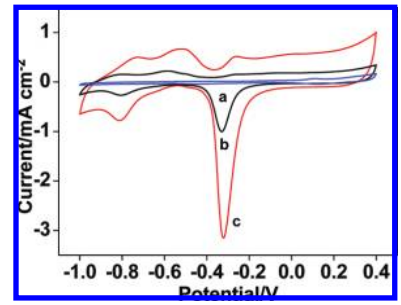

Figure 6. CVs of hollow Au nanospheres (a), Pd nanoparticles (b), and Au/Pd hollow nanostructures (c) modified GC electrode in 0.5 M KOH at the scan rate of 50 mV s^{-1}. The metal loading for each sample is 10 μg.

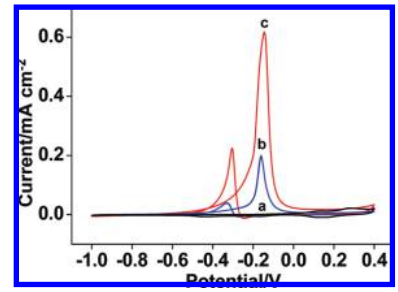

Figure 7. CVs of hollow Au nanospheres (a), Pd nanoparticles (b), and hollow Au/Pd nanostructures (c) modified GC electrode in 0.5 M KOH containing 0.5 M methanol at the scan rate of 50 mV s^{-1}. The metal loading for each sample is 10 μg.

to examine its electrochemical behavior. Figure 6 is the CVs of hollow Au nanospheres (a), Pd nanoparticles (b), and hollow Au/Pd nanostructures (c) modified GC electrode in N_2-saturated 0.5 M KOH at the scan rate of 50 mV s^{-1}. It can be seen that no obvious signals can be observed on hollow Au nanospheres (Figure 6a), whereas Figure 6b shows electrochemical response characteristic of Pd nanoparticles. In Figure 6c, only signals characteristic of Pd are observed, suggesting the original hollow Au nanospheres are covered by a layer of Pd grains, which is in accordance with the explanation by UV−vis spectroscopy. Besides that, response on the as-prepared nanostructure is much larger than that obtained on Pd nanoparticles, indicating the enhanced electrochemical activity exists inside.

It is known that direct methanol fuel cells (DMFCs) have been attracting noticeable attention in recent years. A Pd-based catalyst used as a non-Pt electrocatalyst for methanol oxidation in alkaline media has been proposed.[15] Here, the electroactivity of the prepared raspberry hollow Au/Pd nanostructures was demonstrated. Figure 7 shows the CVs of the prepared nanostructure (c) modified GC electrode comparing with hollow Au nanosphere (a) and Pd nanoparticle (b) modified GC electrodes in 0.5 M KOH containing 0.5 M methanol at the scan rate of 50 mV s^{-1}. From Figure 7c, it can be seen that there is an

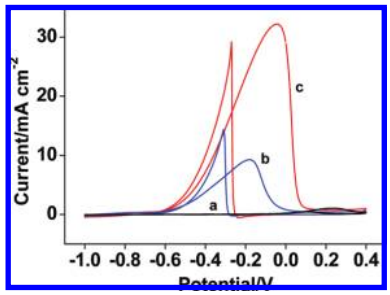

Figure 8. CVs of hollow Au nanospheres (a), Pd nanoparticles (b), and Au/Pd hollow nanostructures (c) modified GC electrode in 0.5 M KOH containing 0.5 M ethanol at the scan rate of 50 mV s^{-1}. The metal loading for each sample is 10 μg.

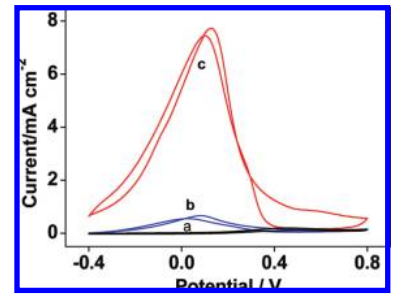

Figure 9. CVs of hollow Au nanospheres (a), Pd nanoparticles (b), and a raspberry hollow Au/Pd nanostructure (c) modified GC electrode in 0.5 M KOH containing 0.5 M formic acid at the scan rate of 50 mV s^{-1}. The metal loading for each sample is 10 μg.

oxidation peak at about −0.12 V (vs. Ag/AgCl) in the forward scan, which is ascribed to the electrooxidation of methanol, and another oxidation peak at around −0.35 V (vs. Ag/AgCl) in the reverse scan, which mainly corresponds to the residual carbon species formed in the forward scan.[48] Similar signals are also obtained on Pd nanoparticle modified GC electrode (Figure 7b), but are several times lower than that acquired on prepared nanostructures. The electroactivity for methanol oxidation of hollow Au nanospheres was also measured. However, no obvious oxidation peaks are observed compared with the prepared nanostructures, as shown in Figure 7a. As a result, the Au/Pd hollow nanostructures exhibit enhanced activity for methanol electrooxidation compared with that of the hollow Au nanospheres or Pd nanoparticles. This enhanced electroactivity may come from the contribution of the combination of hollow Au nanospheres and Pd raspberry nanoshell.

Besides that, ethanol electrooxidation also receives increasing attention since ethanol is less toxic than methanol and can be easily produced in great quantity by the fermentation of sugar-containing raw materials.[7] The Pd-based catalyst used for ethanol electrooxidation in alkaline media has been developed recently.[14,16] Xu and co-workers[16] have found that Pd supported on carbon microspheres even shows excellently higher activity than Pt for ethanol electrooxidation in alkaline media. In this work, the as-prepared hybrid nanostructure was also employed as an electrocatalyst to study its electrochemical behavior of oxidizing ethanol. CVs of ethanol oxidation in 0.5 M KOH containing 0.5 M ethanol on different materials modified GC electrodes at the scan rate of 50 mV s^{-1} are shown in Figure 8. In Figure 8c, we can observe that the onset potential appears at around −0.55 V (vs. Ag/AgCl), a peak in forward scan is at about −0.05 V (vs. Ag/AgCl), and a peak in reverse scan is at about −0.3 V (vs. Ag/AgCl). A Pd nanoparticle modified GC electrode (Figure 8b) also shows similar peaks, but they are much lower, not even half the intensity the hybrid nanostructure exhibits. The bare (not shown) and hollow Au nanosphere modified (Figure 8a) GC electrodes were also examined and no obvious peak was observed. We can conclude that the as-prepared hybrid nanostructure exhibits excellent catalytic property for ethanol electrooxidation in comparison with Pd nanoparticles and hollow Au nanospheres. Experiments on methanol and ethanol oxidation also reveal that the prominent catalytic properties can promote this new electrocatalyst to be applicable in DAFCs.

As a matter of fact, Pd-based catalysts are also found to possess superior performance in formic acid electrooxidation. To the best of our knowledge, carbon supported Pd catalysts usually show well-defined performance in acidic electrolyte.[3−6] The alkaline electrolyte offers us a media employing unsupported Pd-based catalysts. Figure 9 is the CVs of formic acid electrooxidation in 0.5 M KOH containing 0.5 M formic acid on different materials modified GC electrodes at the scan rate of 50 mV s^{-1}. Figure 9c shows the formic acid electrooxidation on the hybrid hollow nanostructure modified GC electrode. Two peaks can be observed at around 0.101 (vs. Ag/AgCl) and 0.128 V (vs. Ag/AgCl) in forward and reverse scan, respectively. It can be seen that the hybrid hollow nanostructure exhibits much better performance than Pd nanoparticles (Figure 9b). In comparison, the hollow Au nanosphere (Figure 9a) and the bare electrode (not shown) were also investigated, and no obvious peak was observed. As mentioned in methanol electrooxidation, the particular structure of the prepared hybrid material should be responsible for the enhanced electroactivty. The hollow cavity first increases the surface-to-volume ratio. The raspberry surface consisted of irregular Pd grains which provides higher surface-to-volume ratio and surface activity, making the electrocatalyst more efficient.

4. Conclusions

Recently, electrooxidation of methanol, ethanol, and formic acid has been attracting much interest due to their potential applications in fuel cells. In this paper, we introduce a raspberry hollow Au/Pd core/shell nanostructure that may be incorporated into fuel cells. This nanostructure is simply fabricated by first fabricating hollow Au nanospheres via a galvanic replacement reaction by using Co nanoparticles as sacrificial template and then coating with a layer of Pd grains to constitute a raspberry surface. By combining several characterizations such as TEM, SEM, XPS, and UV−vis spectroscopy, the product is proved to possess a core/shell nanostructure with a hollow cavity and a raspberry surface. The electrochemical oxidation properties are carried out by cyclic voltammetry. It is found the oxidation signals for methanol, ethanol, and formic acid in alkaline media are all improved in comparison with those of hollow Au nanospheres and Pd nanoparticles. These results may come from the contribution of the combination of the hollow nanostructure and the raspberry surface.

Acknowledgment. This work was supported by the National Natural Science Foundation of China (20775077) and the Chinese Academy of Sciences (KJcx2-YW-H11).

References and Notes

(1) Ganesan, R.; Lee, J. S. *Angew. Chem., Int. Ed.* **2005**, *44*, 6557.
(2) Mu, S. C.; Tang, H. L.; Wan, Z. H.; Pan, M.; Yuan, R. Z. *Electrochem. Commun.* **2005**, *7*, 1143.
(3) Leiva, E.; Iwasita, T.; Herrero, E.; Feliu, J. M. *Langmuir* **1997**, *13*, 6287.
(4) Rice, C.; Ha, S.; Masel, R. I.; Waszczuk, P.; Wieckowski, A.; Barnard, T. *J. Power Sources* **2002**, *111*, 83.

(5) Rhee, Y.-W.; Ha, S. Y.; Masel, R. I. *J. Power Sources* **2003**, *117*, 35.
(6) Bath, B. D.; White, H. S.; Scott, E. R. *Anal. Chem.* **2000**, *72*, 433.
(7) Song, S. Q.; Tsiakaras, P. *Appl. Catal., B* **2006**, *63*, 187.
(8) Steele, B. C. H.; Heinzel, A. *Nature* **2001**, *414*, 345.
(9) Bensebaa, F.; Farah, A. A.; Wang, D. S.; Bock, C.; Du, X. M.; Kung, J.; Le Page, Y. *J. Phys. Chem. B* **2005**, *109*, 15339.
(10) Wang, Y.; Li, L.; Hu, L.; Zhuang, L.; Lu, J.; Xu, B. *Electrochem. Commun.* **2003**, *5*, 662.
(11) Gupta, S. S.; Datta, J. *J. Power Sources* **2005**, *145*, 124.
(12) Tripkovic, A. V.; Popovic, K. D.; Grgur, B. N.; Blizanac, B.; Ross, P. N.; Markovic, N. M. *Electrochim. Acta* **2002**, *47*, 3707.
(13) Guo, D. J.; Li, H. L. *Carbon* **2005**, *43*, 1259.
(14) Shen, P. K.; Xu, C. W. *Electrochem. Commun.* **2006**, *8*, 184.
(15) Sun, Z. P.; Zhang, X. G.; Liang, Y. Y.; Li, H. L. *Electrochem. Commun.* **2009**, *11*, 557.
(16) Xu, C. W.; Cheng, L. Q.; Shen, P. K.; Liu, Y. L. *Electrochem. Commun.* **2007**, *9*, 997.
(17) Nie, S. M.; Emory, S. R. *Science* **1997**, *275*, 1102.
(18) Kim, S. W.; Kim, M.; Lee, W. Y.; Hyeon, T. *J. Am. Chem. Soc.* **2002**, *124*, 7642.
(19) Liang, H. P.; Zhang, H. M.; Hu, J. S.; Guo, Y. G.; Wan, L. J.; Bai, C. L. *Angew. Chem., Int. Ed.* **2004**, *43*, 1540.
(20) Duan, X.; Huang, Y.; Lieber, C. M. *Nano Lett.* **2002**, *2*, 487.
(21) Chan, W. C. W.; Nie, S. *Science* **1998**, *281*, 2016.
(22) Katz, E.; Willner, I. *Angew. Chem., Int. Ed.* **2004**, *43*, 6042.
(23) Zhao, B.; Liu, J.; Liu, Z. R.; Liu, G. X.; Li, Z.; Wang, J. X.; Dong, X. T. *Electrochem. Commun.* **2009**, *11*, 1707.
(24) Sun, Y.; Mayers, B. T.; Xia, Y. *Nano Lett.* **2002**, *2*, 481.
(25) Wang, Y. L.; Cai, L.; Xia, Y. N. *Adv. Mater.* **2005**, *17*, 473.
(26) Lu, L.; Zhang, H.; Sun, G.; Xi, S.; Wang, H.; Li, X.; Wang, X.; Zhao, B. *Langmuir* **2003**, *19*, 9490.
(27) Park, J.-H.; Kim, Y.-G.; Oh, C.; Shin, S.-I.; Kim, Y.-C.; Oh, S.-G.; Kong, S.-H. *Mater. Res. Bull.* **2005**, *40*, 271.
(28) Zhang, J.; Liu, J.; Wang, S.; Zhan, P.; Wang, Z.; Ming, N. *Adv. Funct. Mater.* **2004**, *14*, 1089.
(29) Pol, V. G.; Grisaru, H.; Gedanken, A. *Langmuir* **2005**, *21*, 3635.
(30) Guo, S. J.; Dong, S. J.; Wang, E. K. *Chem.–Eur. J.* **2008**, *14*, 4689.
(31) Sun, Y.; Xia, Y. *J. Am. Chem. Soc.* **2004**, *126*, 3892.
(32) Liang, H. P.; Wan, L. J.; Bai, C. L.; Jiang, L. *J. Phys. Chem. B* **2005**, *109*, 7795.
(33) Schwartzberg, A. M.; Olson, T. Y.; Talley, C. E.; Zhang, J. Z. *J. Phys. Chem. B* **2006**, *110*, 19935.
(34) Chen, M. H.; Gao, L. *Inorg. Chem.* **2006**, *45*, 5145.
(35) Liang, H. P.; Lawrence, N. S.; Wan, L. J.; Jiang, L.; Song, W. G.; Jones, T. G. J. *J. Phys. Chem. C* **2008**, *112*, 338.
(36) Liang, H.; Guo, Y.; Zhang, H.; Hu, J.; Wan, L.; Bai, C. *Chem. Commun.* **2004**, 1496.
(37) Guo, S. J.; Fang, Y. X.; Dong, S. J.; Wang, E. K. *J. Phys. Chem. C* **2007**, *111*, 17104.
(38) Olson, T. Y.; Schwartzberg, A. M.; Orme, C. A.; Talley, C. E.; O'Connell, B.; Zhang, J. Z. *J. Phys. Chem. C* **2008**, *112*, 6319.
(39) Teranishi, T.; Miyake, M. *Chem. Mater.* **1998**, *10*, 594.
(40) Bera, D.; Kuiry, S. C.; McCutchen, M.; Kruize, A.; Heinrich, H.; Meyyappan, M.; Seal, S. *Chem. Phys. Lett.* **2004**, *386*, 364.
(41) Song, J. H.; Kim, F.; Kim, D.; Yang, P. D. *Chem.—Eur. J.* **2005**, *11*, 910.
(42) Glavee, G. N.; Klabunde, K. J.; Sorensen, C. M.; Hadjipanayis, G. C. *Langmuir* **1993**, *9*, 162.
(43) Xiang, Y. J.; Wu, X. C.; Liu, D. F.; Jiang, X. Y.; Chu, W. G.; Li, Z. Y.; Ma, Y.; Zhou, W. Y.; Xie, S. S. *Nano Lett.* **2006**, *6*, 2290.
(44) Liang, H. P.; Lawrence, N. S.; Jones, T. G. J.; Banks, C. E.; Ducati, C. *J. Am. Chem. Soc.* **2007**, *129*, 6068.
(45) Lu, L. H.; Wang, H. S.; Xi, S. Q.; Zhang, H. J. *J. Mater. Chem.* **2002**, *12*, 156.
(46) Ge, Z.; Cahill, D. G.; Braun, P. V. *J. Phys. Chem. B* **2004**, *108*, 18870.
(47) Hu, J. W.; Li, J. F.; Ren, B.; Wu, D. Y.; Sun, S. G.; Tian, Z. Q. *J. Phys. Chem. C* **2007**, *111*, 1105.
(48) Zhu, Y. M.; Uchida, H.; Yajima, T.; Watanabe, M. *Langmuir* **2001**, *17*, 146.

JP905007R